

Control Structure Design and Controllability Analysis for Solid Oxide Fuel Cell

Narissara Chatrattanawet^a, Sigurd Skogestad^b, Amornchai Arpornwichanop^{*a}

^aComputational Process Engineering Research Unit, Department of Chemical Engineering, Faculty of Engineering, Chulalongkorn University, Bangkok 10330, Thailand

^bDepartment of Chemical Engineering, Norwegian University of Science and Technology, 7491 Trondheim, Norway
amornchai.a@chula.ac.th

A solid oxide fuel cell (SOFC) is a highly efficient power generation device. Due to its high-temperature operation, the SOFC can directly run on hydrocarbon fuels which are internally reformed to generate hydrogen within a fuel cell stack. However, the internal reforming causes a temperature gradient in the SOFC stack, especially at the cell inlet. In addition, the coupling of the reforming and electrochemical reactions results in a complicated dynamic response that requires an efficient control system. In this study, the concept of a controllability analysis is applied to the control system design of the SOFC. Controllability plays an important role in designing a control system as it demonstrates the ability to move system outputs to specified bounds using available inputs. Nonlinear dynamic model of the SOFC is used to analyze its steady-state and dynamic behaviour. The obtained results are employed to investigate the controllability properties of the SOFC. To achieve the efficient control system, the control structure of the SOFC is considered.

1. Introduction

A solid oxide fuel cell (SOFC) operates at high temperatures (873-1273 K) and converts the chemical energy in fuels directly to electrical energy by electrochemical reactions (Yamamoto, 2000). The attractive features of fuel cells include no moving parts, quiet operation, low environmental pollution, and high efficiency. Further, it can use various fuel types and the heat generated can be used in the heat and power systems (Varbanov et al., 2009). The direct internal reforming that occurs inside the fuel cell itself is used to convert hydrocarbon fuels into a hydrogen-rich gas. However, the problem with internal reforming is the temperature gradient due to the endothermic cooling effect at the cell inlet.

In recent years, SOFC has received much attention focusing on its operation and design, but less concentration has been given to the control including controllability analysis and control structures design. Controllability analysis can offer insights for identifying the inherent properties of a process and how they limit control performance (Skogestad and Postlethwaite, 1996). Morari (1983) has reported that controllability is an inherent property of the process itself and should be considered at the design stage before the control system design is fixed. The comparison and selection of different control structures and the validation of the controlled system were studied for the controllability analysis of decentralized linear controllers (Garcia et al., 2010). In addition, the controllability analysis is generally applied for selection of the best controlled and manipulated variable pairing within one process and evaluation of control properties for two or more process alternatives. Therefore, the theory of controllability analysis is interesting and challenging for SOFC.

To design efficient control systems, it is necessary to know the structural decisions of control structure design. Control structure design deals with the structural decisions of the control system, including the selection of manipulated variables, controlled variables, control configuration, and controller type and what to control and how to pair the variables to form control loops (Skogestad and Postlethwaite, 1996). Andrade and Lima (2009) concentrated on the control structure design for an ethanol production plant. The proposed structures were tested to verify its performance.

The purpose of this paper is to study the control structure design and controllability analysis of SOFC. The performance of a SOFC with direct internal reforming of methane is also analyzed under steady-state and dynamic behaviours for the selection of the optimal operating point for SOFC. Furthermore, we consider the application of the control structure design procedure of Skogestad (2004) to this process.

2. Solid oxide fuel cell

A sketch of a planar direct internal reforming SOFC (DIR-SOFC) is shown in Figure 1. The structure of solid oxide fuel cells is composed of ceramic ion-conducting electrolyte sandwiched between two porous electrodes, anode and cathode (PEN, Positive electrode-Electrolyte-Negative electrode). When oxygen as oxidant is reduced that occurs on the cathode side and formed into oxygen ions, these ions can diffuse through the ion-conducting electrolyte to the anode/electrolyte interface. Then they react with hydrogen held in the fuel that is supplied continuously to the anode side. The methane as fuel is reformed into hydrogen directly on the anode through the steam reforming reaction and water-gas shift (WGS) reaction. The electrons are produced afterwards via the electrochemical reactions at the anode side. The electrons transport via the external circuit to generate electricity and return to the cathode/electrolyte interface. Water, exhaust gases and heat as by-product are also produced.

3. Mathematical model

The mathematical model of solid oxide fuel cell is based on the mass and energy balances and electrochemical model. The assumptions are considered as follows: (i) steady state and dynamic behaviours are considered; (ii) heat loss to the surrounding is negligible; (iii) all gases are assumed as ideal-gases; (iv) distribution of pressure in the gas channels is negligible; (v) the exit temperatures of fuel and air are same as the cell temperature; (vi) heat capacities are negligible and (vii) lumped-parameter model is considered.

3.1 Mass and energy balances

Methane is assumed that can only be reformed to hydrogen, carbon monoxide, and carbon dioxide and, therefore, not electrochemically oxidized (Aguir et al., 2004). According to the reactions in Table 1, these reactions are used in the mass and energy balances. The lumped-parameter model is implemented to describe the dynamic model and control of the planar SOFC. Lumped-parameter models are adequately accurate for systems-level analysis and control through experimental validation (Xi et al., 2010). The lumped model of the mass balances in the fuel and air channels can be described as:

$$\frac{dn_{i,f}}{dt} = \dot{n}_{i,f}^{in} - \dot{n}_{i,f} + \sum_{k \in \{(i),(ii),(v)\}} \nu_{i,k} R_k A \quad (1)$$

$$\frac{dn_{i,a}}{dt} = \dot{n}_{i,a}^{in} - \dot{n}_{i,a} + \nu_{i,(v)} R_{(v)} A \quad (2)$$

where $\dot{n}_{i,f}$ and $\dot{n}_{i,a}$ are the molar flow rate of species i in the fuel and air channel, respectively. In the fuel channel, subscripts (i) refer to CH_4 , H_2O , CO , H_2 , and CO_2 whereas they refer to N_2 and O_2 in the air channel, $\nu_{i,k}$ is the stoichiometric coefficient of component i in reaction k , R_k is the rate of reaction k , and A is the reaction area.

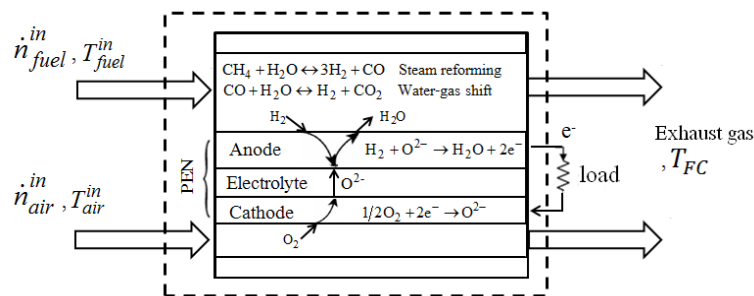


Figure 1: Direct internal reforming solid oxide fuel cell

Table 1: Reactions considered in a SOFC

Reaction name	No.	Reaction equation
steam reforming	(i)	$\text{CH}_4 + \text{H}_2\text{O} \leftrightarrow 3\text{H}_2 + \text{CO}$
water-gas shift	(ii)	$\text{CO} + \text{H}_2\text{O} \leftrightarrow \text{H}_2 + \text{CO}_2$
hydrogen oxidation	(iii)	$\text{H}_2 + \text{O}^{2-} \rightarrow \text{H}_2\text{O} + 2\text{e}^-$
oxygen reduction	(iv)	$1/2\text{O}_2 + 2\text{e}^- \rightarrow \text{O}^{2-}$
Overall cell	(v)	$\text{H}_2 + 1/2\text{O}_2 \rightarrow \text{H}_2\text{O}$

It is assumed that the temperature variation inside the cell is negligible for the lumped model of energy balance. The fuel cell temperature (T_{FC}) can be found by Eq(3),

$$\frac{dT_{FC}}{dt} = \frac{1}{\rho_{SOFC} C_{pSOFC} V_{SOFC}} \left(\dot{Q}_{f,in} - \dot{Q}_{f,out} + \dot{Q}_{a,in} - \dot{Q}_{a,out} + \sum_{k \in \{(i),(ii),(v)\}} (-\Delta H)_k R_k A - j A V_{FC} \right) \quad (3)$$

$$\dot{Q}_i = \sum_j \dot{n}_j C_{p_j} (T_i - T_{ref}) \quad (4)$$

which ρ_{SOFC} , C_{pSOFC} , and V_{SOFC} represent the density, heat capacity, and volume of SOFC, respectively and ΔH represents the heat of reaction, \dot{Q}_i shows the enthalpy flow, and subscripts i and j in Eq(4) refer to the corresponding streams (fuel or air) and components, respectively.

The rate expression of the steam reforming reaction ($R_{(i)}$) is given in Achenbach et al. (1994). Excess steam is used to prevent carbon formation on the catalyst and to force the reaction to completion. An associated reaction to the reforming reaction is the water-gas shift reaction. Unlike the steam reforming reaction, the water gas-shift reaction is an exothermic reaction. The rate expression of water gas shift reaction ($R_{(ii)}$) is given in Herberman and Young (2004). According to Faraday's law, the overall cell reaction ($R_{(v)}$) is related to the electric current density (j).

3.2 Electrochemical model

The theoretical open-circuit voltage (E_{OCV}) is the maximum voltage which depends on the gas composition and temperature at the electrodes and occurs from the difference between the thermodynamic potentials of the electrode reactions. It can be found by the Nernst equation and shown as Eq(5).

$$E_{OCV} = E_0 - \frac{RT_{FC}}{2F} \ln \left(\frac{p_{\text{H}_2\text{O}}}{p_{\text{H}_2} p_{\text{O}_2}^{0.5}} \right) \quad (5)$$

where E_0 is the open-circuit potential at the standard pressure and is a function of the operating temperature that can be expressed by Eq(6) and p_i is the partial pressure of component i .

$$E_0 = 1.253 - 2.4516 \times 10^{-4} T_{FC} \text{ (K)} \quad (6)$$

When an external load is connected, the operating cell voltage or the actual voltage (V_{FC}) decreases from its open-circuit voltage due to ohmic losses, concentration overpotentials, and activation overpotentials.

$$V_{FC} = E_{OCV} - (\eta_{Ohm} + \eta_{conc} + \eta_{act}) \quad (7)$$

The ohmic losses (η_{Ohm}) occur when the oxide ions diffuse through the electrolyte, the electrons transport through the porous electrodes, and contact resistance occurs between cell components. It can also be obtained based on the Ohm's law as follows:

$$\eta_{Ohm} = j R_{Ohm} \quad (8)$$

where R_{Ohm} is the internal resistance of the cell that involves resistivity and thicknesses of electrodes and electrolyte. It is also calculated from the conductivity of the individual layers.

$$R_{\text{Ohm}} = \frac{\tau_{\text{anode}}}{\sigma_{\text{anode}}} + \frac{\tau_{\text{electrolyte}}}{\sigma_{\text{electrolyte}}} + \frac{\tau_{\text{cathode}}}{\sigma_{\text{cathode}}} \quad (9)$$

where τ_{anode} , $\tau_{\text{electrolyte}}$, and τ_{cathode} refer to the thickness of the anode, electrolyte, and cathode layers, respectively, σ_{anode} and σ_{cathode} refer to the electronic conductivity of the anode and cathode, respectively, and $\sigma_{\text{electrolyte}}$ refers to the ionic conductivity of the electrolyte.

The concentration overpotentials (η_{conc}) can be caused when the reactants are consumed by the electrochemical reaction faster than diffusing into the porous electrode and can also be caused by variation in bulk flow composition, which causes a drop in the local potential near the end of the cell. The concentration overpotentials can be calculated by Eq(10).

$$\eta_{\text{conc}} = \frac{RT_{FC}}{2F} \ln \left(\frac{p_{\text{H}_2\text{O,TPB}} p_{\text{H}_2}}{p_{\text{H}_2\text{O}} p_{\text{H}_2,\text{TPB}}} \right) + \frac{RT_{FC}}{4F} \ln \left(\frac{p_{\text{O}_2}}{p_{\text{O}_2,\text{TPB}}} \right) \quad (10)$$

where $p_{i,\text{TPB}}$ is the partial pressure of component i at three-phase boundaries (TPB).

The result of the kinetics involved with the electrochemical reactions is the activation overpotentials (η_{act}). The equation shown below is estimated by solving the non-linear Butler-Volmer equation, which relates the current density drawn to the activation overpotentials.

$$j = j_{0,\text{anode}} \left[\frac{p_{\text{H}_2,\text{TPB}}}{p_{\text{H}_2}} \exp \left(\frac{\alpha n F}{RT_{FC}} \eta_{\text{act,anode}} \right) - \frac{p_{\text{H}_2\text{O,TPB}}}{p_{\text{H}_2\text{O}}} \exp \left(- \frac{(1-\alpha) n F}{RT_{FC}} \eta_{\text{act,anode}} \right) \right] \quad (11)$$

$$j = j_{0,\text{cathode}} \left[\exp \left(\frac{\alpha n F}{RT_{FC}} \eta_{\text{act,cathode}} \right) - \exp \left(- \frac{(1-\alpha) n F}{RT_{FC}} \eta_{\text{act,cathode}} \right) \right] \quad (12)$$

where α is the transfer coefficient and usually taken to be 0.5, n is the number of electrons transferred in the single elementary rate-limiting reaction step. The exchange current density of electrode ($j_{0,\text{electrode}}$) can be expressed by:

$$j_{0,\text{electrode}} = \frac{RT_{FC}}{nF} k_{\text{electrode}} \exp \left(- \frac{E_{\text{electrode}}}{RT_{FC}} \right), \text{ electrode} \in \{\text{anode, cathode}\} \quad (13)$$

where the activation energy of the electrode exchange current densities ($E_{\text{electrode}}$) and the pre-exponential factor of the electrode exchange current densities ($k_{\text{electrode}}$) are given by Aguiar et al. (2004).

4. Behavior of SOFC

The understanding of steady-state and dynamic behaviour is an essential necessity for the nonlinear control system design. In this study, the optimal operating points at steady state condition is selected at current density = 0.5 A/cm², the cell voltage = 0.72 V, the power density = 0.36 W/cm², and the cell temperature = 1,069 K (see Figure 2). After optimum designs are obtained, open-loop dynamic responses to step changes around the assumed operating point are investigated. In Figure 3, the responses of the cell temperature and cell voltage are shown for a 10 % increase in current density, inlet temperature of air and fuel, and velocity of air and fuel. The cell operating temperature and fuel cell voltage are dependent on the fuel and air inlet temperature as well as the current density.

5. Control structure design

The most important control structure decision is usually to identify good controlled variables (CVs). And to find the active constraints, which should be controlled to operate the plant optimally is interesting. We here follow the stepwise procedure of Skogestad (2004).

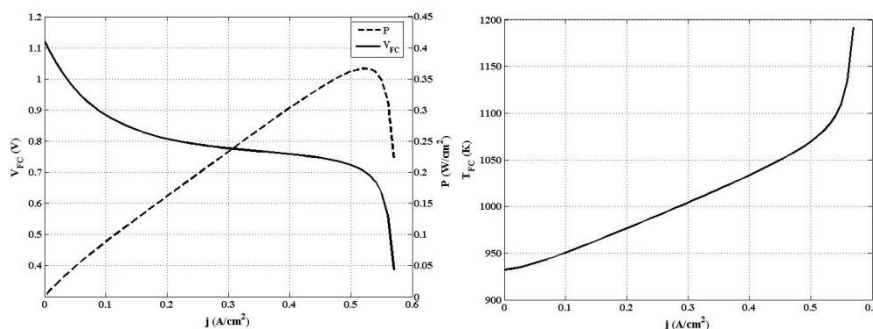


Figure 2: The cell voltage, power density and the cell temperature as a function of the current density at the steady-state for a planar SOFC

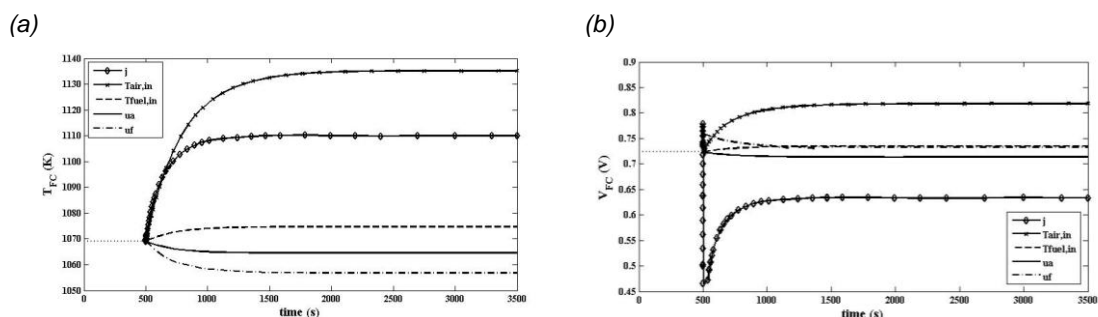


Figure 3: The responses of (a) the cell temperature and (b) the cell voltage due to step changes of 10% in five different input

Step 1: Define cost J and constraints. With a given load (current density), the cost function J to be minimized is the cost of the fuel feed minus the value of the power, subject to satisfying constraints on the cell temperature kept at 1,069 K.

Step 2: Identify optimal operation as a function of disturbances. At steady-state, there are two operational degrees of freedom; the inlet molar flow rate of air and fuel, $MV = [\dot{n}_{air}^{in}, \dot{n}_{fuel}^{in}]$. The current density (j) is the main disturbance, and it is also the throughput manipulator (TPM) for the system. We have optimized the system in detail, the fuel cell temperature constraint of $T_{FC} = 1,069$ K is assumed to always be active. There is then one remaining unconstrained degree of freedom, which is related to the excess of air.

Step 3: Identify economic CVs. We select $CV = [T_{FC}, x_{CH_4}]$. The first CV is the active constraints. As a “self-optimizing” variable for the unconstrained degree of freedom we select the fraction of unconverted methane in the exhaust gas (x_{CH_4}) which was found to result in a small economic loss.

Step 4: The throughput manipulator is already mentioned the current density.

Step 5: Structure of stabilizing control layer. An important decision here is to select the “stabilizing” controlled variables CV2, including inventories and other drifting variables that need to be controlled on a short time scale. In this case, one need to control temperature tightly to avoid material stresses and one need to prevent cell voltage drop due to depletion of fuel. Fortunately, in this case the economic controlled variables (CV1) are also acceptable as stabilizing variables (CV2=CV1), so a separate regulatory layer is not needed.

Step 6: Select structure for control of CV1. This is the pairing issue which is discussed in Section 6 on “controllability analysis”.

6. Controllability analysis (Choice of pairing)

The controllability of a process is the ability to achieve acceptable control performance; that is, to preserve the outputs with in specified bounds. It offers a numerical indication of the sensitivity balance to provide a qualitative assessment of the control properties of the alternative designs. In this work, relative gain array (RGA) is performed as the controllability index for the selection of control pairing and to describe the interactions among inputs and output. Generally, the RGA formed in the gain matrix close to the unity matrix are preferred but control structures with high RGA elements should be avoided. The RGA of a non-

singular square complex matrix (G) is defined as indicated in Eq(14), where \times denotes element by element multiplication (the Hadamard or Schur product).

$$\text{RGA}(G) = \Lambda(G) = G \times (G^{-1})^T \quad (14)$$

The selection of the controlled and manipulated variables for the investigated system is analyzed at the control structure design part. To perform the controllability analysis of DIR-SOFC, we consider the lumped-parameter models with the inlet molar flow rates of air (u_1) and fuel (u_2). The fuel cell temperature (y_1) and the fraction of methane (y_2) are selected as outputs.

The steady-state RGA is 1.94 for the diagonal pairings (u_1 - y_1 , u_2 - y_2), which is close to 1 as desired. This pairing is also reasonable from a dynamic point of view because the molar flow rate of fuel at inlet (u_2) has a direct effect on the fraction of methane (y_2).

7. Conclusions

This work focuses on a control structure design and controllability analysis of SOFC operated under a direct internal reforming of methane. The dynamic response of SOFC in terms of the fuel cell voltage and cell temperature are investigated following the step change in the operating conditions such as the inlet temperatures of air and fuel and current density. The result shows the inlet air temperature and current density are the main disturbances that affect the cell temperature and cell voltage. The control structure design is implemented to identify good controlled variable. We found the cell temperature is the active constraints that should be controlled at its setpoint. Moreover, the fraction of unconverted methane is a good CV for the remaining unconstrained variable by the self-optimizing concept. According to the RGA, the result shows the inlet molar flow rates of air and fuel are manipulated variable to control the cell temperature and the concentration of fuel, respectively.

Acknowledgements

Support from The Royal Golden Jubilee PhD Program, The Thailand Research Fund and the National Research University, Office of Higher Education Commission (WCU-040-EN57) is gratefully acknowledged.

References

- Achenbach E., Riensche E., 1994, Methane/steam reforming kinetics for solid oxide fuel cells. *Journal of Power Source*, 52, 283-288.
- Aguiar P., Adjiman C.S., Brandon N.P., 2004, Anode-supported intermediate temperature direct internal reforming solid oxide fuel cell I: model-based steady-state performance. *Journal of Power Sources*, 138, 120-136.
- Andrade G.V.N., Lima E.L., 2009, Control structure design for an ethanol production plant. 10th International Symposium on Process Systems Engineering, 27, 1551-1556.
- Garcia V.M., Lopez E., Serra M., Llorca J., Riera J., 2010, Dynamic modeling and controllability analysis of an ethanol reformer for fuel cell application. *International Journal of Hydrogen Energy*, 35, 9768-9775.
- Morari M., 1983, Flexibility and resiliency of process systems. *Computers & Chemical Engineering*, 7, 423-437.
- Skogestad S., 2004, Control structure design for complete chemical plants. *Computers and Chemical Engineering*, 28, 219-234.
- Skogestad S., Postlethwaite I., 1996, *Multivariable Feedback Control, Analysis and Design*. John Wiley&Sons, New York.
- Varbanov P., Frierler F., 2009, Boosting energy conversion efficiency using fuel cells. SOFC-ST assessment using the EMINENT tool. *Chemical Engineering Transaction*, 18, 117-122.
- Xi H., Varigonda S., Jing B., 2010, Dynamic modeling of a solid oxide fuel cell system for control design. *American Control Conference (ACC)*, 423-428.
- Yamamoto O., 2000, Solid oxide fuel cells: fundamental aspects and prospects. *Electrochimica Acta*, 45, 2423-2435.